Progress In Electromagnetics Research, Vol. 141, 537–552, 2013

A BIDIRECTIONAL CIRCULARLY POLARIZED ARRAY OF THE SAME SENSE BASED ON CRLH TRANSMISSION LINE

Wendong Liu, Zhijun Zhang*, and Zhenghe Feng

Department of Electronic Engineering, Tsinghua University, Beijing, China

Abstract—A bidirectional circularly polarized array of the same sense is proposed. The implementation is a combination of end-fire array, crossed dipoles, and composite right/left-handed transmission line (CRLH-TL). The proposed array consists of four dipoles spaced at a distance equal to $\lambda_0/4$ (λ_0 is the wavelength in free space at the center frequency). For the bidirectional circular polarization of the same sense, the four dipoles are fed in-phase in a series-fed structure. A feed line that exhibits 0° phase shift every $\lambda_0/4$ is needed. To satisfy the demand for the space distance and phase distribution in a series-fed array, the CRLH unit cell composed of lumped capacitors and inductors is employed and inserted in the feed line. Theoretical analysis is performed based on the balanced parallel stripline and design equations are presented for the determination of the lumped element parameters. The design method can be used in the design of the arrays with more elements. From the experimental results, the array offers a 4.2 dBic bidirectional circular polarization gain. The bandwidth between which the impedance matching is better than -10 dB and the axial-ratio is better than 3 dB is 300 MHz from 2.39 to 2.69 GHz.

1. INTRODUCTION

In cases such as tunnels, long streets, or long bridges, communicable cells are formed along these areas. The size of the microcell zones can be efficiently increased by using bidirectional antennas, which preferentially radiate the antenna beam along the longitude [1, 2]. Linear polarized bidirectional antennas [3–9] have been studied and

Received 28 May 2013, Accepted 29 July 2013, Scheduled 1 August 2013

* Corresponding author: Zhijun Zhang (zjzh@tsinghua.edu.cn).

introduced. However, polarization mismatch becomes a problem when the antennas are not aligned in practical application. Thus, bidirectional circularly polarized antenna is quite suitable for the base station in relay communication. Another advantage is that for the mobile units or sensors in such a link, linear polarization antenna is quite sufficient, thus reducing system complexity and cost. Roughly, bidirectional circularly polarized antenna can be classified into two types: Slot type [10–12] and wire type [13–15]. The way of producing circular polarization (CP) is to excite two orthogonal linearly polarized components in the same plane with the same amplitude and a 90° phase difference. However, the bidirectional senses of both types are not the same. Such antennas are not suited for communication between relay stations because the senses of the receiving antenna and the transmitting antenna are destined to be opposite. So bidirectional circularly polarized antenna of the same sense is needed. To realize this goal, the traditional solution is to combine two circularly polarized unidirectional antennas back to back. However, such techniques need additional feed network, which makes the structure not compact. A slot-coupled back-to-back microstrip antenna was proposed in [16] where two corner-cutting CP patches were arranged relative to a slot on the ground plane. Limited impedance and AR bandwidths are observed due to the patch mode. To achieve higher gain, more patch antenna elements and larger ground plane is needed, which results in larger cross-section. This may be a potential drawback in the applications that low profile is required. On the other hand, for bidirectional radiation, the realized gain suffers from 3 dB loss compared to that of the original unidirectional antennas such as patch antenna in [16].

Recently, studies of left-handed (LH) meta-materials have progressed rapidly. From a practical application standpoint, the transmission line approach of LH meta-materials has led to the realization of composite right/left-handed transmission line (CRLH-TL). The CRLH-TL has many unique properties such as supporting a fundamental backward wave (opposite group and phase velocities) and zero propagation constant with nonzero group velocity at the zeroth-order resonance. Application based on CRLH-TL such as antennas [17, 18] and microwave components [19, 20] have been proposed.

In this paper, we propose, design, and experimentally verify a four-element-array for bidirectional circular polarization. The sense of circular polarization is the same in both axial directions. The solution is to combine two end-fire dipole arrays orthogonally at a distance of $\lambda_0/4$. The main challenge is to feed all the dipoles in-

phase in a series-fed structure. To satisfy the demand, a CRLH-TL composed of lumped capacitors and inductors is constructed, which exhibits 0° phase shift every $\lambda_0/4$. The employed CRLH-TL is based on the balanced parallel stripline. Theoretical analysis is performed and design equations are presented for the determination of the lumped element parameters. Details of the array design are presented, and simulation and measurement results are also presented and discussed.

2. ANTENNA CONFIGURATION AND ANALYSIS

In this section, the working principle of the proposed array and CRLH-TL are presented.

2.1. Bidirectional Circular Polarization of the Same Sense

The principle of bidirectional circular polarization of the same sense is shown in Fig. 1. It consists of two in-phase crossed dipoles separated in space by $\lambda_0/4$. The 90° phase difference between the two orthogonal electric field components is caused by the distance ($\lambda_0/4$) in space, which is distinct from the common way. In $+z$ direction, the phase of the electric field component radiated from dipole I has a lead of 90° and vice versa. Thus LHCP are generated in both axial directions. Similarly, RHCP can be generated by exchanging the positions of the two dipoles or exciting the two dipoles with 180° phase difference. The problem is that the radiation pattern $f_1(\theta, \varphi)$ of the two crossed dipoles looks more like an oblique dipole and is not bidirectional. Obviously, this is caused by the omnidirectional pattern of dipoles. Thus the solution is to replace the omnidirectional dipole with a bidirectional antenna. In other words, it is to combine two bidirectional linearly

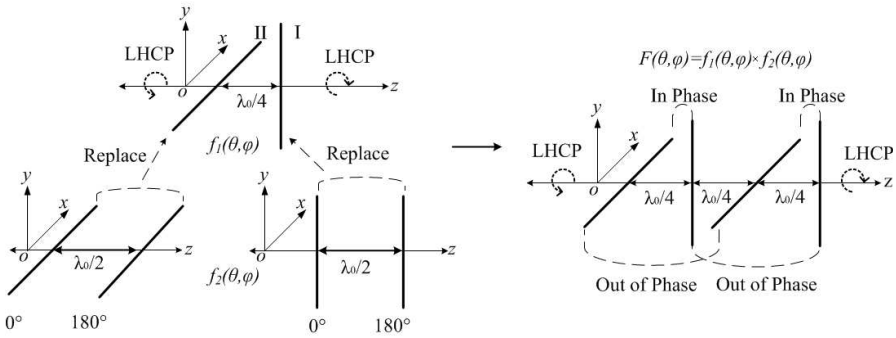

Figure 1. The principle of bidirectional circular polarization of the same sense.

polarized antennas orthogonally at a distance of $\lambda_0/4$. In this paper, a bidirectional dipole array with a radiation pattern $f_2(\theta, \varphi)$ is chosen as shown in Fig. 1. The adjacent elements are spaced by $\lambda_0/2$ and excited with 180° phase difference. Thus the radiation pattern of the proposed array $F(\theta, \varphi)$ should be:

$$F(\theta, \phi) = f_1(\theta, \phi) \times f_2(\theta, \phi) \tag{1}$$

As a result, the distance between adjacent elements in the array is $\lambda_0/4$ as shown in Fig. 1. It should be noted that the design method can be used in the design of the arrays with more elements. The number of the array elements must be an integral multiple of 4.

2.2. Composite Right/Left-handed Transmission Line

As mentioned above, the spacing between array elements is fixed because it affects the bidirectional radiation property and circular polarization property. Moreover, 0° phase shift is needed between the points spaced by $\lambda_0/4$. This is a challenge for traditional right-handed transmission line (RH-TL). The CRLH-TL, due to its special phase velocities property, can be used to achieve the special phase distribution. The equivalent circuit of the non-radiating CRLH-TL is shown in Fig. 2, which is demonstrated and studied in detail in [21]. It is the combination of an LH-TL and a RH-TL. The LH-TL consists of lumped elements, which is the series capacitor C_L and parallel inductor L_L. The RH-TL is the conventional balanced parallel stripline with a total length L of $\lambda_0/4$, which just equals the spacing between the array elements. The phase shift for the LH-TL and RH-TL are φ_{LHTL} and φ_{RHTL}, respectively. Mathematically, the total phase shift φ_{total} across the CRLH-TL satisfies the following equation

$$\varphi_{total} = \varphi_{RHTL} + \varphi_{LHTL} = L\beta_{TL} + \varphi_{LHTL} \tag{2}$$

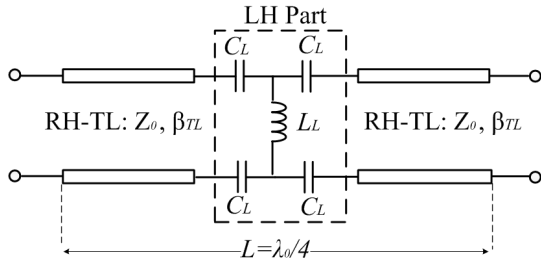

Figure 2. Equivalent lumped elements circuit model for CRLH-TL.

where β_{TL} is the propagation constant of the host TL. The LH-TL exhibits positive phase response (phase lead) and can compensate the negative phase response (phase lag) induced by the nature of RH-TL. 0° phase shift between the two ports can be predicted. Due to the special structure, analysis based on network parameter is performed which is different from that in [21]. Equation (3) gives the $[A\,B\,C\,D]$ matrix for the LH part in the dash box shown in Fig. 2 as

$$\begin{aligned} A &= \begin{bmatrix} 1 & aZ \\ 0 & 1 \end{bmatrix} \begin{bmatrix} 1 & 0 \\ Y & 0 \end{bmatrix} \begin{bmatrix} 1 & aZ \\ 0 & 1 \end{bmatrix} = \begin{bmatrix} 1 & a\frac{1}{j\omega C_L} \\ 0 & 1 \end{bmatrix} \begin{bmatrix} 1 & 0 \\ \frac{1}{j\omega L_L} & 0 \end{bmatrix} \begin{bmatrix} 1 & a\frac{1}{j\omega C_L} \\ 0 & 1 \end{bmatrix} \\ &= \begin{bmatrix} 1 - \frac{a}{\omega^2 L_L C_L} & \frac{a}{j\omega C_L}\left(2 - \frac{a}{\omega^2 L_L C_L}\right) \\ \frac{1}{j\omega L_L} & 1 - \frac{a}{\omega^2 L_L C_L} \end{bmatrix} \rightarrow S_1 = \begin{bmatrix} S_{11} & S_{12} \\ S_{21} & S_{22} \end{bmatrix} \end{aligned} \tag{3}$$

where S_1 represents the S-parameter matrix corresponding to A. For balanced TL such as the balanced parallel stripline in this work, the parameter "a" equals to 2. For an unbalanced TL such as microstrip line, the parameter "a" equals to 1. There are two degrees of freedom C_L and L_L, thus certain constraint on the reflection coefficient is reasonable besides the demand for the angle of S_{21}. On the other hand, the behavior that is expected from the proposed CRLH-TL should be the same as a phase shifter, which means that the S-parameter matrix that is expected should be

$$S_0 = \begin{bmatrix} 0 & e^{j\theta} \\ e^{j\theta} & 0 \end{bmatrix} = S_1 \tag{4}$$

θ represents the phase shift between the two ports. Since S_1 and S_0 represent the same circuits, S_1 should be equal to S_0. After calculation, the L_L and C_L can be found as:

$$\begin{cases} L_L = \dfrac{Z_0}{\omega_0 \sin\theta} \\ C_L = \dfrac{2}{Z_0 \omega_0 \tan(\theta/2)} \end{cases} \tag{5}$$

To validate the theory, simulation based on the full-wave simulator HFSS and calculated results based on circuit model have been performed. The models are shown in Figs. 3(a) and (b). The central frequency is chosen to be 2.5 GHz and the corresponding $\lambda_0/4$ is 30 mm. The transmission line is the balanced parallel stripline with a width of 3 mm. The substrate used is a low-cost teflon with a dielectric constant $\varepsilon_r = 2.65$ and a thickness of 1 mm, which makes the simulated characteristic impedance Z_0 58.2 Ω and the simulated guided wavelength λ_g 83.6 mm. The size of the lumped elements is chosen to be $1 \times 0.5\,\text{mm}^2$. The length left to transmission line is 28 mm,

which will induce $-120°$ phase shifter. Thus, for $0°$ phase shift, the parameter θ is set to be $120°$. According to (5), the corresponding parameters can be found to be $L_L = 4.1\,\text{nH}$, $C_L = 1.2\,\text{pF}$. As shown in Fig. 3(b), $120°$ phase shift is obtained from the circuit model regardless of the transmission line. However, a little adjustment around the ideal lumped element values is needed in the simulation by HFSS, which results in $L'_L = 3.8\,\text{nH}$, $C'_L = 1.08\,\text{pF}$. Such result is not surprising because the parameters calculated from (5) are obtained from pure circuit model, where ideal TEM mode and no discontinuity are assumed. In full wave simulation, all the above factors need to be taken into consideration which makes the results accurate. Thus all the following simulation and experiments are based on full wave simulation. Equation (5) still gives a guideline for theoretical analysis and initial design.

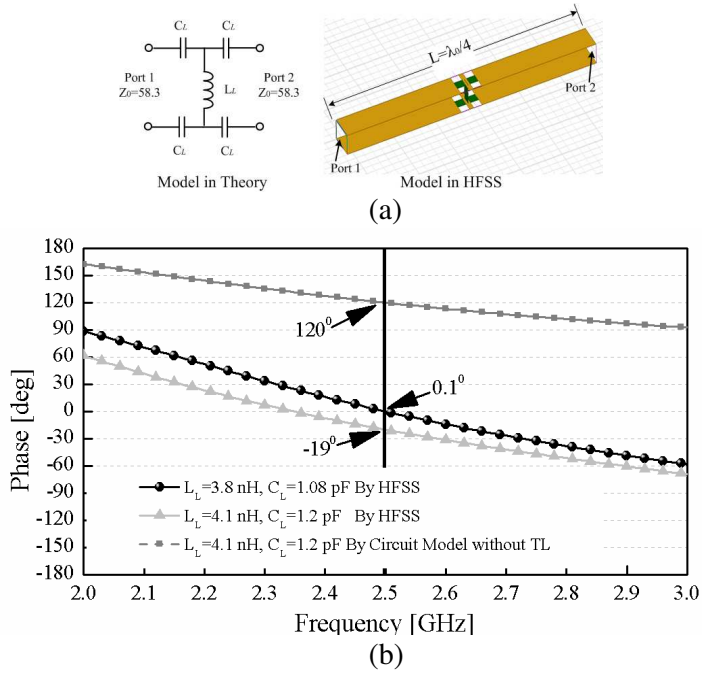

Figure 3. (a) Circuit model without TL and simulated model in HFSS. (b) Phase shift varied with frequency.

From the above, it is concluded that such this CRLH-TL can achieve any phase shift without any reflection at ports, which is the same as ideal phase shifter. Equation (5) combines only the characteristic impedance of the RH-TL, the phase shift required, and

the values of L_L and C_L. Thus there is no need to calculate the per-unit-length reactance of the RH-TL. Actually, the equivalent circuit model above is not an ideal CRLH-TL but a quasi CRLH-TL in some degree. For an ideal CRLH-TL working at the state ($\beta_{CRLH} = 0$), the phase shift between any two points on the CRLH-TL is 0°. However, in the model used in this paper, 0° phase shift can only be achieved between specific two points.

3. ANTENNA DESIGN

Based on the above analysis, a four-element-array is designed and shown in Fig. 4. It consists of four dipoles spaced at a distance equal to $\lambda_0/4$, a balanced parallel stripline, and two LH unit cells. The array is fed from the center. The benefit is that element A_1 and B_1 is in phase naturally. It would cut down the quantity of the lumped elements and increase the array efficiency. On the other hand, the radiation property and the energy distribution would be more symmetric. Due to the CRLH-TL, all the elements now can be fed in phase. To obtain 180° phase difference between elements A_1 and A_2 (B_1 and B_2), the connection types need to be adjusted as shown in Fig. 4(b). Fig. 5

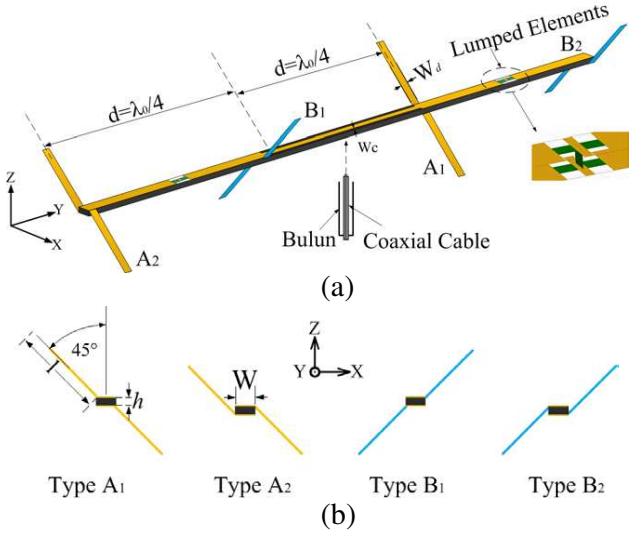

Figure 4. (a) 3-D view of the proposed array. (b) Side view of the four types of dipole. Values of the parameters are $d = 30$, $h = 1$, $l = 28$, $W = 3$, $W_d = 3$, $W_C = 0.5$ (unit: millimeter).

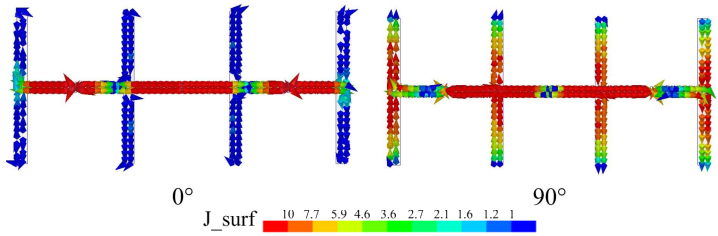

Figure 5. Distribution of the surface current on the feed line and the array at 2.5 GHz in 0° and 90° phase.

shows the vector current distributions of the proposed array at 2.5 GHz viewed from the $+z$-direction. All the currents resonate in the same rhythm and correspond to the theoretical analysis above. Note that the current distribution in 180° and 270° are equal in magnitude and opposite in phases 0° and 90°.

All the parameters of the transmission line are set to be same as mentioned in Section 2, which means $w = 3\,\text{mm}$, $\varepsilon_r = 2.65$, and $h = 1\,\text{mm}$. The value of h is chosen according to the size of shunt inductor used because the inductors need to be just buried in the transmission line in practice. The length of the dipoles is chosen to be 28 mm nearly $\lambda_0/4$ at 2.5 GHz and the width of the dipoles is chosen to be 3 mm.

The equivalent circuit for the series-fed array is shown in Fig. 6(a). Due to symmetry, only half of the circuit is shown. Port 1 represents the central feed point. Ports 2 and 3 represent the dipoles A_1 and B_2. The special transfer characteristic of the circuit varied with the values of the series capacitors C_L and shunt inductors L_L is studied by Microwave Office. Actually, the specific characteristic impedance of the three ports doesn't affect the general variation trend of the circuit. Neither does the length and width of the TL between Ports 1 and 2. All the parameters in the dash box are the same as mentioned before. Fig. 6(b) shows the influence of the shunt inductors L_L. The phase difference between port 2 and 3 is small and changes slowly with L_L except when L_L is quite small and the shunt inductor tends to be a short circuit element. Though the magnitude of S_{21} and S_{31} changes with L_L drastically, the difference between them is quite small in a wide range. The influence of series capacitor C_L is shown in Fig. 6(c). Both the magnitude and phase of S_{21} and S_{31} change with C_L. It should be noted that the optimal L_L and C_L (3 dB power divider and 0° phase shift) are just the values given by (4). The influence of L_L and C_L on current distribution, axial-ratio and directivity of

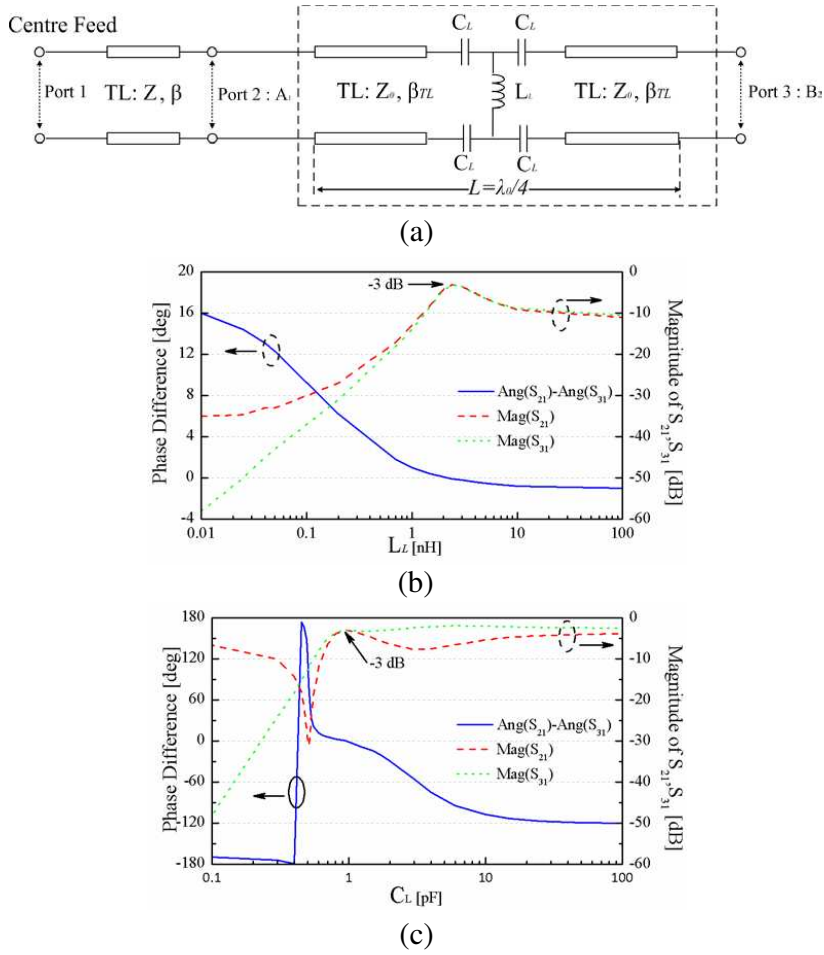

Figure 6. (a) Equivalent circuit for the series-fed array (half). (b) S-parameter varied with L_L. (C) S-parameter varied with C_L.

the proposed array is further studied and confirmed by the full-wave simulator HFSS. The current distribution varied with L_L is shown in Fig. 7(b). When L_L deviates from the optimal value, all the elements resonate almost in phase. However, the energy that each dipole gets drops down synchronously. Thus, as shown in Fig. 7(a), the axial-ratio and CP directivity is almost invariable as L_L is tuned. The influence of series capacitors C_L is shown in Fig. 8. Both the phase and magnitude of the current variations are observed when C_L deviates from the optimal value significantly. Thus the directivity drops as C_L

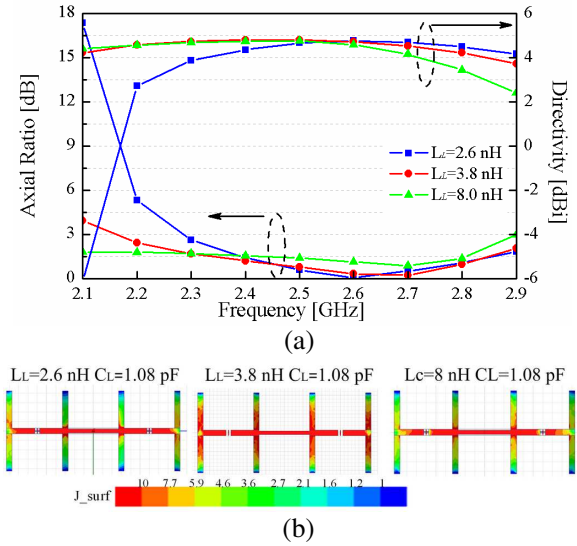

Figure 7. The influence of L_L. (a) Axial-ratio and directivity. (b) Current distribution.

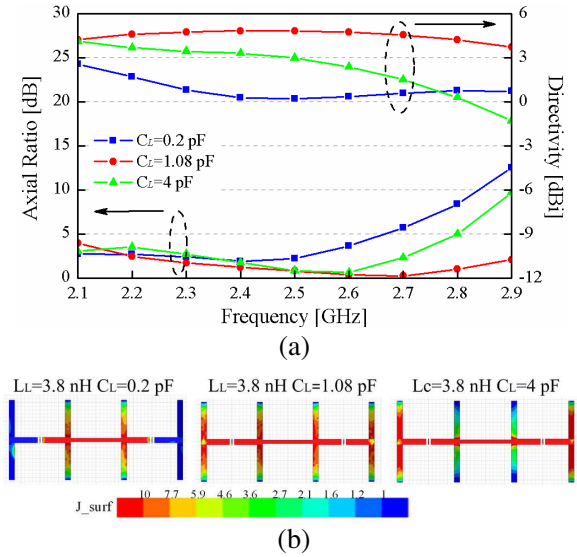

Figure 8. The influence of C_L. (a) Axial-ratio and directivity. (b) Current distribution.

varies. Due to symmetry, B_1 and A_1 are always in phase and so are B_2 and A_2. Moreover, the two groups generate the same CP wave in both axial directions. Thus, the axial ratio is almost invariable as L_L and C_L vary as shown in Figs. 7 and 8. Good agreement between circuit simulation and full wave simulation is obtained. Naturally, the impedance seen from the feeding point can be matched to $50\,\Omega$ by adjusting the radiation impedance of the dipole element (L_d and W_d). However, the optimal matching frequency point deviates from 2.5 GHz. To tackle this problem, the section of the transmission line in the middle is replaced by a narrower one with higher characteristic impedance. As shown in Fig. 9, the impedance curve is moved from the left side (low impedance part) of the smith chart to centre and the matching frequency is just at 2.5 GHz.

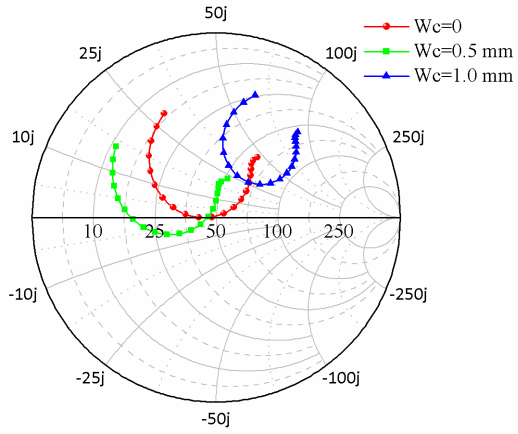

Figure 9. Port impedance varied with W_C.

The simulated axial-ratio beams varied with frequency in the x-y plane and y-z plane are shown in Fig. 10. A wider 3 dB beam width is observed in the x-y plane.

4. EXPERIMENTAL RESULTS

The four-element bidirectional circularly polarized array of the same sense presented in Section 3 is fabricated and tested experimentally. The photograph of the simple prototype is shown in Fig. 11. The substrate of the parallel stripline is low-cost telfon with dielectric constant of $\varepsilon_r = 2.65$ and height of 1 mm. In this paper, the sizes of all SMT chip components, provided by the Murata Manufacturing Company Ltd., Kyoto, Japan, are $1.0 \times 0.5\,\text{mm}^2$ (0402). There are

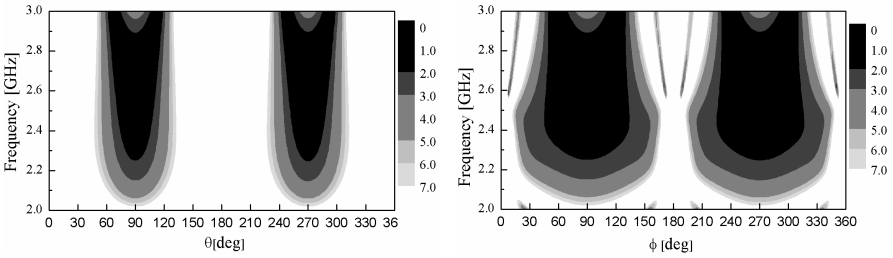

Figure 10. Simulated axial-ratio beams varied with frequency. (a) *yoz* plane. (b) *xoy* plane.

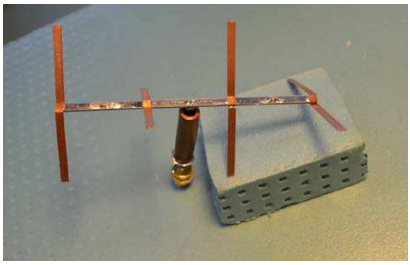

Figure 11. Photograph of the realized prototype.

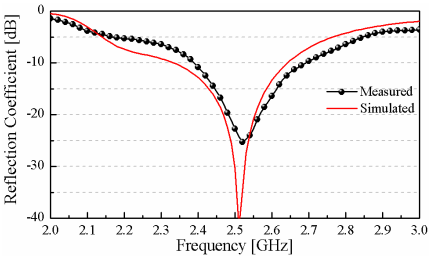

Figure 12. Simulated and measured reflection coefficients of the proposed array.

only limited available values of inductance/capacitance of SMT chip components, and parasitic effects of the SMT chip components at 2.5 GHz have to be considered. Therefore, the values of L_L and C_L in the fabricated circuit are slightly different from that in the design, which results in $L_L = 3.6$ nH and $C_L = 1.2$ pF. Fig. 12 shows the simulated and measured reflection coefficient of the fabriccirated array. The measured 10 dB return loss bandwidth is 300 MHz (2.39–2.69 GHz) and the simulated is 320 MHz (2.34–2.66 GHz). A good agreement between the simulated results and the measured results is obtained. To verify that the proposed array has a bidirectional circularly polarized radiation pattern, the radiation characteristics of the prototype were also studied. The AR is measured using a spinning linear method where a rotating linearly polarized transmit horn antenna is used to measure the CP performance of the antenna. The measured and simulated AR at two end of the array is shown in Fig. 13. The measured 3 dB AR bandwidth is about 730 MHz (2.16–2.89 GHz) and it is much wider than the return loss bandwidth. The simulated 3 dB AR bandwidth is 850 MHz (2.15–3 GHz). The measured 3 dB AR variation with

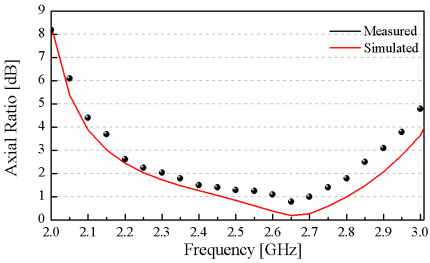

Figure 13. Simulated and measured ARs in the axial direction ($\pm y$).

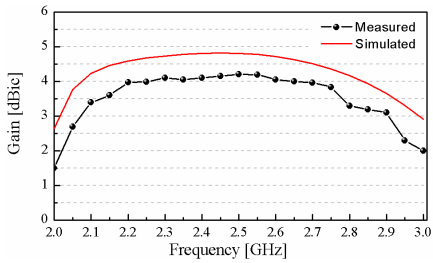

Figure 14. Simulated and measured gains in the axial direction ($\pm y$).

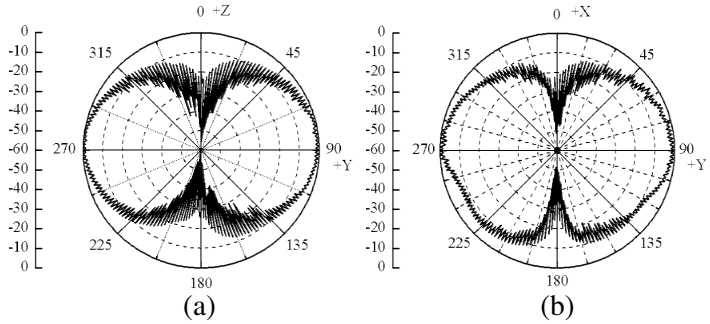

Figure 15. Measured spinning normalised AR patterns of the array at 2.5 GHz. (a) *yoz* plane. (b) *xoy* plane.

frequency agrees well with the simulated results. Fig. 14 shows the measured and simulated bidirectional gain of the array. Actually, there is a slight difference between the gains in the axial directions due to the errors in measurement and fabrication. Thus, only the maximum gain is given. The measured maximum gain is 4.2 dBic at 2.5 GHz and the simulated maximum gain is 4.9 dBic at 2.45 GHz. Besides the error in measurement, the drop of the gain is mainly induced by the losses of the lumped elements used at 2.5 GHz, which is a little beyond the optimal working frequency range. Shown in Fig. 15 is the far field pattern of the proposed array at 2.5 GHz. The slight discrepancy between the AR patterns in the x-y and y-z planes are due to the antenna installation error in an anechoic chamber, when the antenna is mounted for the x-y and y-z planes on AUT stand. The array is fed at the center by a coaxial cable. A balun is needed to accomplish the transition between the balanced parallel stripline and the unbalanced coaxial line. The current on the balun itself which is induced by the radiation fields from the dipoles is small and can be ignored.

5. CONCLUSION

The concept of a bidirectional circularly polarized array with the same sense at both axial ends was theoretically and experimentally investigated in this paper. The proposed array consists of two bidirectional dipole array, which are assigned orthogonally and spaced by $\lambda_0/4$. The CRLH-TL composed of lumped capacitors and inductors is employed to satisfy the demand for the space distance and phase distribution in a series-fed array. To practically realize the previous concept, a four-element array was proposed, designed, and tested experimentally. From the experimental results, the array offers a 4.2 dBic bidirectional circular polarization gain and the bandwidth between which the impedance matching is better than -10 dB and the axial-ratio is better than 3 dB is about 300 MHz from 2.39–2.69 GHz. The proposed concept also serves as a guideline for the design with more elements to realize higher gain. The proposed array is quite suitable for relay communication in long and narrow areas such as long streets, tunnels, or bridges.

ACKNOWLEDGMENT

This work is supported by the National Basic Research Program of China under Contract 2010CB327400, in part by the National Natural Science Foundation of China under Contract 60771009, the National High Technology Research and Development Program of China (863 Program) under Contract 2009AA011503, the National Science and Technology Major Project of the Ministry of Science and Technology of China 2010ZX03007-001-01, and Tsinghua-QUALCOMM associated Research Plan.

REFERENCES

1. Hori, T., K. Cho, and K. Kagoshima, "Bidirectional base station antenna illuminating a street microcell for personal communication system," *Proc. Antennas Propag. Soc. Int. Symp.*, Vol. 1, 419–422, 1995.
2. Freman, R. L., "Radio system design for telecommunication," Ch. 10, McGraw-Hill, New York, 2007.
3. Krairiksh, M., P. Keowsawat, C. Phongcharoenpanich, and S. Kosulvit, "Two-probe excited circular ring antenna," *Progress In Electromagnetics Research*, Vol. 97, 417–431, 2009.
4. Zhang, J., X. M. Zhang, J. S. Liu, Q. F. Wu, T. Ying, and H. Jin, "Dual-band bidirectional high gain antenna for WLAN

2.4/5.8 GHz applications," *Electronics Letters*, Vol. 45, 6–7, Jan. 2009.

5. Mahatthanajatuphat, C., P. Akkaraekthalin, S. Saleekaw, and M. Krairiksh, "A bidirectional multiband antenna with modified fractal slot fed by CPW," *Progress In Electromagnetics Research*, Vol. 95, 59–72, 2009.
6. Iwasaki, H., "Microstrip antenna with back-to-back configuration relative to a slot on a ground plane," *Electronics Letters*, Vol. 34, 1373–1374, Jul. 1998.
7. Chen, S.-Y., "Broadband slot-type bruce array fed by a microstrip-to-slotline T-junction," *IEEE Antennas Wireless Propag. Lett.*, Vol. 8, 116–119, 2009.
8. Lamultree, S. and C. Phongcharoenpanich, "Full-wave investigations of a probe-excited rectangular ring antenna by method of moments with RWG basis functions," *Progress In Electromagnetics Research C*, Vol. 8, 161–177, 2009.
9. Azim, R. and M. T. Islam, "Compact planar UWB antenna with band-notch characteristics for WLAN and DSRC," *Progress In Electromagnetics Research*, Vol. 133, 391–406, 2013.
10. Chen, C. and E. K. N. Yung, "Dual-band dual-sense circularly-polarized CPW-fed slot antenna with two spiral slots loaded," *IEEE Trans. on Antennas and Propag.*, Vol. 57, No. 6, 1829–1833, 2009.
11. Rezaeieh, S. A. and M. Kartal, "A new triple band circularly polarized square slot antenna design with crooked T and F-shape strips for wireless applications," *Progress In Electromagnetics Research*, Vol. 121, 1–18, 2011.
12. Sze, J.-Y. and S.-P. Pan, "Design of broadband circularly polarized square slot antenna with a compact size," *Progress In Electromagnetics Research*, Vol. 120, 513–533, 2011.
13. Bolster, M. F., "A new type of circular polarizer using crossed dipoles," *IRE Transactions on Microwave Theory and Techniques*, Vol. 5, No. 9, 385–388, 1961.
14. Chi, L.-P., S.-S. Bor, S.-M. Deng, C.-L. Tsai, P.-H. Juan, and K.-W. Liu, "A wideband wide-strip dipole antenna for circularly polarized wave operations," *Progress In Electromagnetics Research*, Vol. 100, 69–82, 2010.
15. Wang, C.-J. and C.-H. Lin, "A circularly polarized quasi-loop antenna," *Progress In Electromagnetics Research*, Vol. 84, 333–348, 2008.

16. Lwasaki, H. and N. Chiba, "Circularly polarised back-to-back microstrip antenna with an omnidirectional pattern," *IEE Proc. Microw. Antennas Propag.*, Vol. 146, No. 4, 277–281, 1999.
17. Nordin, M. A. W., M. T. Islam, and N. Misran, "Design of a compact ultrawideband metamaterial antenna based on the modified split-ring resonator and capacitively loaded strips unit cell," *Progress In Electromagnetics Research*, Vol. 136, 157–173, 2013.
18. Yu, A., F. Yang, and A. Z. Elsherbeni, "A dual band circularly polarized ring antenna based on composite right and left handed metamaterials," *Progress In Electromagnetics Research*, Vol. 78, 73–81, 2008.
19. Jimenez-Martin, J. L., V. Gonzalez-Posadas, J. E. Gonzalez-Garcia, F. J. Arques-Orobon, L. E. Garcia-Munoz, and D. Segovia-Vargas, "Dual band high efficiency class ce power amplifier based on CRLH diplexer," *Progress In Electromagnetics Research*, Vol. 97, 217–240, 2009.
20. Huang, J.-Q. and Q.-X. Chu, "Compact UWB band-pass filter utilizing modified composite right/left-handed structure with cross coupling," *Progress In Electromagnetics Research*, Vol. 107, 179–186, 2010.
21. De Vincentis, M., C. Caloz, and T. Itoh, "Arbitrary dual-band components using composite right/left-handed transmission lines," *IEEE Trans. on Microwave Theory and Tech.*, Vol. 52, No. 4, 1142–1149, 2004.